Int J Adv Manuf Technol (2015) 76:1783–1792
DOI 10.1007/s00170-014-6400-8

ORIGINAL ARTICLE

Study on surface roughness in high-speed milling of AlMn1Cu using factorial design and partial least square regression

Z. H. Wang · J. T. Yuan · T. T. Liu · J. Huang · L. Qiao

Received: 16 October 2012 / Accepted: 16 September 2014 / Published online: 26 September 2014

Abstract Anti-rust aluminum is widely used in aviation, aerospace, communications, as well as weapons with non-corrosion, light, and other fine characteristics. In this study, in order to improve the machined surface quality and find the functional relation between cutting parameters and surface roughness, a series of cutting experiments for AlMn1Cu were conducted, and the surface roughness values in high-speed milling were obtained. Firstly, according to the analysis of variance (ANOVA) of factorial experiments, the cutting parameters significantly influencing the surface roughness were presented. Secondly, the mathematical prediction models of surface roughness based on the cutting parameters were established by using the partial least squares regression. Finally, experiments are further designed and carried out to validate the accuracy of the proposed prediction model.

Keywords Surface roughness · Cutting parameters · AlMn1Cu · Factorial design · Partial least square regression

1 Introduction

The functional parts made by anti-rust aluminum alloy have been widely used in aviation, aerospace, communications, as well as weapons with non-corrosion, light, and other fine characteristics in recent years. In general, the functional parts need higher surface quality in order to achieve certain functional behavior. For the anti-rust aluminum alloy, the machined cavity's surface has a lot of defects such as burr, furrow, etc. And the machined surface quality is difficult to meet the technical specifications due to its low strength and high softness. So, the problem on how to improve the machined cavity's surface quality for anti-rust aluminum alloy is necessary to be solved.

Surface roughness is an important indicator to reflect the surface quality. The surface roughness formation mechanism along with the numerous uncontrollable factors that influence pertinent phenomena makes it almost impossible with a simple solution to reveal the nature of cutting surface. The common strategy involves the selection of conservative process parameters, which neither guarantees the achievement of the desired surface roughness nor attains high metal removal rate [1].

In the recent 20 years, there have been numerous studies conducted on the prediction of surface roughness and the optimization of cutting parameters for many engineering applications. As for the theoretical and empirical models about surface roughness and cutting parameters, Geoffrey and Winston presented the theoretical arithmetic idealized model of arithmetical mean value R_a for turning operation. A lot of empirical regression models for surface roughness based on the cutting parameters were proposed [2]. Fang and Safi-Jahanshaki presented a new algorithm to establish a reference tool-based model for predicting the surface roughness through the correlation analysis and regression method. Compared with the traditional method, the algorithm needed much less experimental work, but it showed a reasonable accuracy in predicting the surface roughness in finish machining [3]. Hasan et al. developed a Taguchi optimization method for low surface roughness in terms of process parameters when milling the mold

Z. H. Wang (✉) · J. T. Yuan · T. T. Liu · J. Huang · L. Qiao
School of Mechanical Engineering, Nanjing University of Science and Technology, 200 Xiao Ling Wei Street, Nanjing 210094, Jiangsu, People's Republic of China
e-mail: niatwzh17@163.com

Table 1 Mechanical properties of AlMn1Cu

Tensile strength (MPa)	Yield strength (MPa)	Hardness (HB)	Elasticity modulus (GPa)
130	50	300	71

surfaces of 7075-T6 aluminum material [4]. Chen and Lee developed an on-line surface recognition system that was based on a statistical multiple regression model, and sensing techniques were used to monitor the effects of vibration produced by the motions of the cutting tool and workpiece during turning operations. Test results indicated that the system could predict surface roughness on line and in real time with an approximate accuracy of 94 % [5]. The mathematical models of aluminum alloy 2014 were presented for predicting five different surface profile parameters caused by internal ball burnishing process parameters, namely burnishing speed, feed, depth of penetration, and number of passes [6]. Erol et al. study the influence machining parameters on the surface roughness obtained in drilling of AISI 1045 and developed a mathematical prediction model of the surface roughness using response surface methodology (RSM) [7]. Wang et al. presented a theoretical and experimental investigation into the effect of the workpiece material on surface roughness in the ultra-precision milling process and studied the influences of material swelling and tool-tip vibration on surface generation in ultra-precision raster milling [8]. Cakir et al. examined the effects of cutting parameters (cutting speed, feed rate, and depth of cut) on the surface roughness through the mathematical model developed by using the data gathered from a series of turning experiments performed [9]. Chinnasamy and Muthu carried out the machining process on brass C26000 material in dry cutting condition in a CNC turning machine and presented an artificial neural network (ANN) model that has been designed through

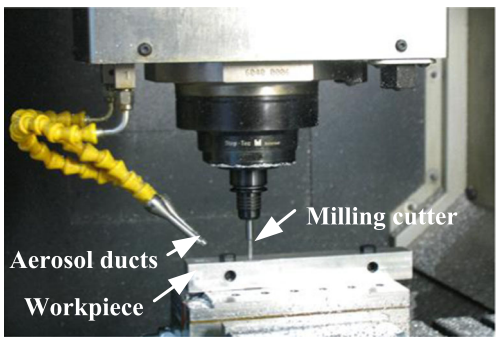

Fig. 1 The experimental setup

feedforward back-propagation network using Matlab (2009a) software to predict the surface roughness [10]. An actual modeling approach using a feed forward multilayered neural network for the prediction and control of surface roughness in turning has been investigated [11]. A neural network-based surface roughness Pokayoke system with in-process NN-based surface roughness prediction system was used to predict the roughness in end milling and to adjust the machine parameters on line when a defect of surface roughness was detected by the system [12]. Öktem developed an integrated study of surface roughness to model and optimize the cutting parameters in the end milling of AISI 1040 steel material with TiAlN solid carbide tools under the wet cutting condition and presented an artificial neural network (ANN) based on back-propagation (BP) learning algorithm to construct the surface roughness model by a full factorial design of experiments [13]. Lee et al. presented an abductive network for modeling drilling process to predict the surface roughness [14]. Çolak et al. used evolutionary programming methods to predict surface roughness in end milling aluminum 6061-T8 [15]. Ding et al. investigated the effects of cutting parameters on cutting forces and surface roughness in hard milling of AISI H13 steel with coated carbide tools and found that the axial depth of cut and the feed were the two dominant factors affecting the cutting forces and established two empirical models for predicting the cutting forces and surface roughness [16]. Basak et al. discussed the burnishing parameters which affect to surface roughness and surface hardness on aluminum 7075-T6 materials and used a fuzzy model based on the experimental results to achieve the best parameters for the burnishing process [17]. Oktem et al. developed a neural network model to predict the surface roughness in the mold cavity and used genetic algorithm coupled with neural network to find optimum cutting parameters leading to minimum surface roughness without any constraint [18]. Bozdemir and Aykut developed an artificial neural network (ANN) model to predict the surface roughness of Castamide block samples in wet and dry conditions [19]. Palani and Natarajan presented a system for automated, noncontact, and flexible prediction of surface roughness of end-milled parts through a machine vision system which is integrated with an artificial neural network (ANN) [20]. Dhokia et al. showed the use of GA to formulate an optimized surface roughness prediction model for ball-end machining of polypropylene [21]. A RBF neural network model was used to predict the surface roughness in turning stainless steel 304L [22]. Benardos et al. presented a feed forward artificial neural network to predict the surface roughness (R_a) in

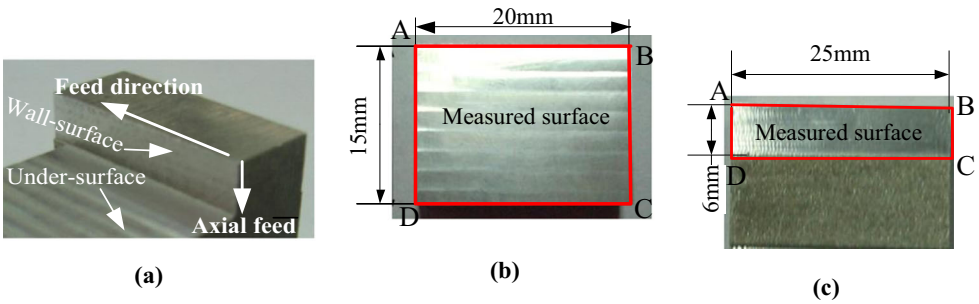

Fig. 2 **a** Machined specimen, **b** testing specimen and critical region of $R_{a,u}$, and **c** testing specimen and critical region of $R_{a,w}$

CNC face milling series 2 aluminum alloy [23]. Çaydaş et al. developed a feed forward neural network based on back-propagation and a regression model to predict surface roughness in the abrasive water jet machining process [24]. Artificial neural network models were developed for the analysis and prediction of the relationship between the cutting conditions and the corresponding fractal parameters of machined surface in face-milling operation [25].

The literatures revealed that the study which focused on the high intensity and hardness materials had achieved a wealth of fruit on surface roughness. But few researches were reported on the low strength and soft materials, such as anti-rust aluminum alloy. In the presented paper, the effects of cutting parameters on the surface roughness were studied for improving the machined surface quality of anti-rust aluminum (AlMn1Cu) in high-speed milling. The high-speed machining (HSM) is widely applied in modern manufacturing to produce exact structural parts and functional parts in aerospace and weapon industries with high machining efficiency, lower cutting forces, higher part precision, and better surface quality. So, the surface quality of the aluminum alloy parts is significantly improved by the high-speed machining technology.

This paper aims to study the cutting parameters significantly affecting the surface roughness as well as to build the prediction model of the surface roughness based on the cutting parameters such as cutting speed, feed-per-tooth, and depth of cut. For those purposes, the experiments were designed on the basis of the factorial design and homogeneous design methodology.

Table 2 The cutting parameters and their levels used in the factorial design experiment

Cutting parameter	Level 1	Level 2	Level 3
Cutting speed, v_c [m/min]	100.54	301.63	502.72
Feed per tooth, f_z [mm/tooth]	0.03	0.05	0.07
Depth of cut, a_p [mm]	0.5	1.5	2.5

2 Experimental works

2.1 Experimental conditions

Milling experiments were conducted using a high-speed machining center (Mikron Corporation, model: XSM600), whose maximum spindle speed is 60,000 rpm and maximum feed rate is 85 m/min. The workpiece material used for the experiments is AlMn1Cu whose chemical composition includes Si 0.6 %, Fe 0.7 %, Cu 0.2 %, Mn 1.0~1.6 %, Mg 0.05 %, Zn 0.1 %, and Ti 0.15 % in addition to Al. The mechanical properties of AlMn1Cu are given in Table 1. The dimension of the workpiece is 150 mm×25 mm×25 mm. The milling cutter is 4-mm diameter two-flute end mill H10F uncoated carbide tool supplied by SANVIK (Code, R216.32-04030-AC08P). The experimental setup is shown in Fig. 1.

2.2 Surface roughness measurements

The arithmetic mean value (R_a) is the most popular method to describe surface roughness in engineering practice. Mathematically, R_a is the arithmetic value of the departure of the profile from centerline along sampling length. In this paper, the R_a is selected to describe the surface roughness.

The end milling is capable of producing two kinds of surfaces: under surface and wall surface. The under-surface is produced on the end mill's end cutting edge, and the wall surface is produced on the end mill's cylindrical cutting edge, as shown in Fig. 2a. In this paper, the under-surface and wall

Table 3 The cutting parameters and their levels used in the homogeneous design experiment

Cutting parameter	Level 1	Level 2	Level 3	Level 4	Level 5
Cutting speed, v_c [m/min]	100.54	201.09	301.63	402.18	502.72
Feed per tooth, f_z [mm/tooth]	0.03	0.04	0.05	0.06	0.07
Depth of cut, a_p [mm]	0.5	1.0	1.5	2.0	2.5

Table 4 The experimental results of factorial design for R_a

No.	v_c [m/min]	f_z [mm/tooth]	a_p [mm]	$R_{a,u}$ [μm]	$R_{a,w}$ [μm]
1	100.54	0.03	0.5	0.260	0.326
2	301.63	0.03	0.5	0.213	0.255
3	502.72	0.03	0.5	0.181	0.237
4	100.54	0.05	0.5	0.284	0.423
5	301.63	0.05	0.5	0.226	0.344
6	502.72	0.05	0.5	0.253	0.296
7	100.54	0.07	0.5	0.391	0.828
8	301.63	0.07	0.5	0.353	0.369
9	502.72	0.07	0.5	0.399	0.414
10	100.54	0.03	1.5	0.254	0.524
11	301.63	0.03	1.5	0.429	1.578
12	502.72	0.03	1.5	0.375	2.046
13	100.54	0.05	1.5	0.378	0.305
14	301.63	0.05	1.5	0.557	2.129
15	502.72	0.05	1.5	0.417	2.392
16	100.54	0.07	1.5	0.533	0.683
17	301.63	0.07	1.5	0.557	1.873
18	502.72	0.07	1.5	0.446	2.687
19	100.54	0.03	2.5	0.311	0.349
20	301.63	0.03	2.5	0.653	2.802
21	502.72	0.03	2.5	0.514	1.658
22	100.54	0.05	2.5	0.449	0.253
23	301.63	0.05	2.5	0.662	2.391
24	502.72	0.05	2.5	0.639	3.182
25	100.54	0.07	2.5	0.602	0.535
26	301.63	0.07	2.5	0.874	2.748
27	502.72	0.07	2.5	0.624	3.245

surface were measured by utilizing a portable surface profilometer (MarSurfPS1). The surface roughness (R_a) of the under-surface is quoted as $R_{a,u}$. Fig. 2b shows the testing specimen and critical region (ABCD) of $R_{a,u}$. The surface roughness (R_a) of the wall surface is quoted as $R_{a,w}$. Fig. 2c shows the testing specimen and critical region (ABCD) of $R_{a,w}$. Roughness measurements (the cutoff is 0.8 mm) were repeated at least five times, and the average of five R_a value was presented.

2.3 Experiment design

For investigating the effects of cutting parameters (spindle speed N, feed per tooth f_z, and depth of cut a_p) on the surface roughness and building the predictive mathematic model of surface roughness by the least squares regression, series of experiments were conducted. Firstly, a 3^3 (3 factors, 3 levels, 27 tests) full factorial design was used for the end milling experiments. The milling parameters were shown in Table 2. Secondly, the homogeneous design was used for the experiments. The levels for the milling parameters with respect to the homogeneous design experiments were shown in Table 3. All milling operations for workpieces were conducted with the conventional milling at a width of cut $w=2.5mm$.

3 Results and discussion

3.1 Factorial design experiments

The factorial design experiment was carried out in order to research the influence of the cutting speed (v_c, m/min), feed per tooth (f_z, mm/z), and depth of cut (a_p, mm) on the surface roughness (R_a). The experimental results were listed in Table 4. The range analysis of factorial experiment indicates that the minimum $R_{a,u}$ and $R_{a,w}$ are all achieved at $v_c=502.72m$/min, $f_z=0.03$ mm/tooth, and $a_p=0.5$ mm. In this experimental conditions, the same cutting experiments were carried out four times, the $R_{a,u}$ is within 0.145~0.187 μm and the $R_{a,w}$ is within 0.210~0.245 μm.

The analysis of variance (ANOVA) was used to study cutting parameters significantly affecting the surface roughness. The significance levels of F tests are selected as $\alpha_1=0.01$ and $\alpha_2=0.05$. The symbol '**' indicates that the corresponding source is significant at 0.99 confidence level, and the symbol '*' indicates that the corresponding source is significant at 0.95 confidence level. Table 5 shows the result of ANOVA for $R_{a,u}$. It can be concluded that the significant

Table 5 ANOVA for $R_{a,u}$

Source of variance	Sum of squares	Degrees of freedom	Mean square	F value	C%	
v_c	0.0642	2	0.0321	5.177	7.92	*
f_z	0.1413	2	0.0707	11.403	17.44	**
a_p	0.4257	2	0.2128	34.322	52.53	**
$v_c \times f_z$	0.0102	4	0.0026	0.419	1.26	–
$v_c \times a_p$	0.0802	4	0.0200	3.225	9.90	–
$f_z \times a_p$	0.0249	4	0.0062	1.000	3.07	–
e (error)	0.0639	8	0.0080	1.290	7.88	–
Total	0.8104	26	–	–	100	–
e'	0.0990	16	0.0062	–		–

SS sum of squares, *DF* degrees of freedom, *MS* mean square, *C%* percent contribution for SS_{Total}

$F_{0.99,2,16}=6.226$, $F_{0.99,4,16}=4.773$, $F_{0.95,2,16}=3.634$, $F_{0.95,4,16}=3.007$, $ss_{e'} = ss_e + ss_{f_z \times a_p} + ss_{v_c \times f_z}$

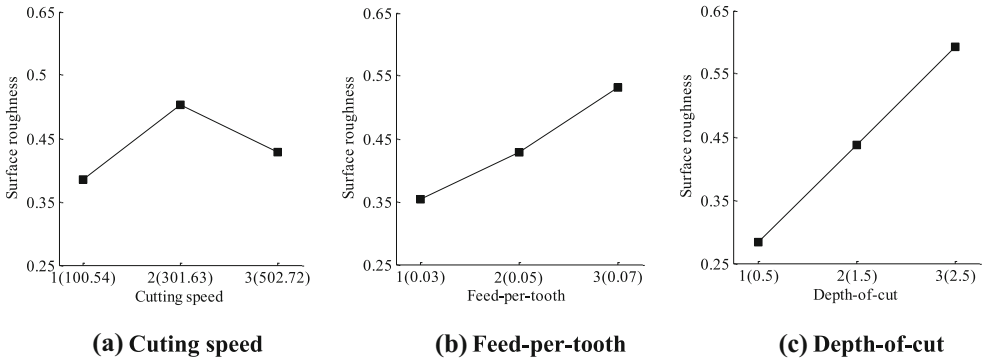

Fig. 3 Main effects plots for $R_{a,u}$

factors affecting $R_{a,u}$ are the depth of cut, feed per tooth, cutting speed, and the interaction between cutting speed and depth of cut. The depth of cut is the most statistically significant factor influencing $R_{a,u}$, which explains 52.53 % of the total variances. The second largest contribution comes from the feed per tooth with 11.403 %.

The main effects of cutting speed, feed per tooth, and depth of cut for $R_{a,u}$ are plotted in Fig. 3. The main effect plots are just graphs of the response averages at the levels of the three factors. Fig. 3a shows that the average of $R_{a,u}$ is larger at v_c= 301.63 m/min (the spindle speed (N) is 24,000 rpm), because the forced regenerative chatter of milling cutter is prone to occur at N=24,000 rpm and the large a_p. Figure 4 shows the machined surface obtained in two different depths of cut at the same spindle speed and feed per tooth. As shown, an increase in depth of cut led to slight milling cutter chatter. $R_{a,u}$ increases with the increase of feed per tooth and depth of cut (Fig. 3b, c). Figure 5 presents the three-dimensional surface plot of $R_{a,u}$ response. When the depth of cut is 0.5 mm, $R_{a,u}$ decreases with the increase of cutting speed and increases with the increase of the feed per tooth (Fig. 5a). When the depth of cut is 1.5 and 2.5 mm, the values of $R_{a,u}$ are larger at v_c= 301.63 m/min (N=24,000 rpm). Therefore, the preconditions to obtain the smaller values of surface roughness should avoid the cutting parameters which induce the forced regenerative chatter of milling cutter.

Table 6 shows the result of ANOVA for $R_{a,w}$. It can be concluded that the significant factors affecting $R_{a,w}$ are the

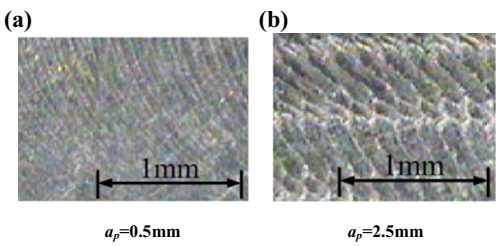

Fig. 4 The photomicrographs of machined under surface with the different a_p (N=24,000 rpm, f_z=0.07 mm/tooth)

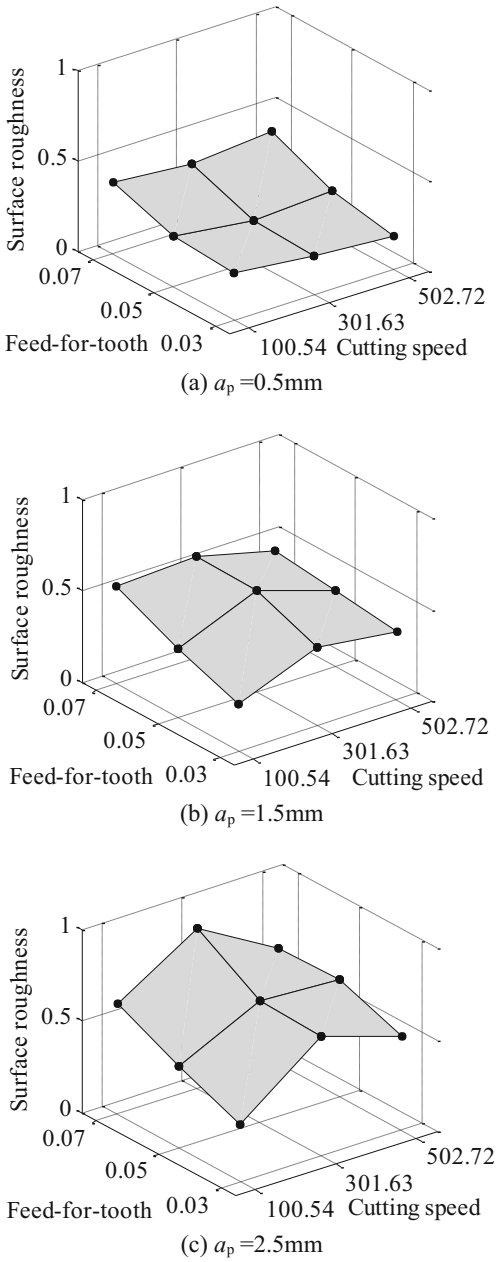

Fig. 5 The effects of spindle speed and feed per tooth on $R_{a,u}$ in different depth of cut

Table 6 ANOVA for $R_{a,w}$

Source of variance	Sum of squares	Degrees of freedom	Mean square	F value	$C\%$	
v_c	9.2763	2	4.6382	41.747	30.71	**
f_z	0.7242	2	0.3621	3.259	2.40	–
a_p	11.5037	2	5.7519	51.772	38.08	**
$v_c \times f_z$	0.5897	4	0.1474	1.327	1.95	–
$v_c \times a_p$	6.9236	4	1.7309	15.580	22.92	**
$f_z \times a_p$	0.0682	4	0.0171	0.154	0.23	–
e (error)	1.1203	8	0.0140	0.126	3.71	–
Total	30.206	26	–	–	100	–
e'	1.7782	16	0.1111	–		–

SS sum of squares, *DF* degrees of freedom, *MS* mean square, *C%* percent contribution for SS_{Total}

$F_{0.99,2,16}$=6.226, $F_{0.99,4,16}$=4.773, $F_{0.95,2,16}$=3.634, $F_{0.95,4,16}$=3.007, $ss_{e'} = ss_e + ss_{f_z \times a_p} + ss_{v_c \times f_z}$

depth of cut, cutting speed, and interaction between cutting speed and depth of cut. The depth of cut is the most statistically significant factor influencing $R_{a,w}$, which explains 38.08 % of the total variances. The second largest contribution comes from the cutting speed with 30.71 %, and the feed per tooth does not have statistical significance for $R_{a,w}$.

Figure 6 shows the same result with the analysis of variance. For the main factors, the feed per tooth affects the surface roughness less, while the depth of cut and cutting speed are the significant factors affecting the surface roughness ($R_{a,w}$). The surface roughness appears to be a non-linear increasing function of v_c and a_p and to be an almost-linear increasing function of f_z. This result seems to contradict with a common expectation that the surface roughness usually decreases with the increase of cutting speed. At this point, it should be due to the interaction between cutting parameters. The milling cutter flutter is prone to occur when the cutting parameters are at a higher level. So, the deeper cutting marks and large plastic deformation are generated on the machined surface, and the surface roughness is greatly increased. Figure 7 shows the relationship between the surface roughness and the cutting parameters. When a_p is 0.5 mm, the values of surface roughness, which are small, decrease with increasing cutting speed. But, when the depth of cut is 1.5 and 2.5 mm, the values of surface roughness are greatly increased with the increase of cutting speed. In addition, it can be concluded from Fig. 7 that the values of surface roughness slightly increase with feed per tooth increasing at the same cutting speed and depth-of-cut. Therefore, the conditions to obtain the smaller values of surface roughness are high cutting speed, small feed per tooth, and small depth of cut.

3.2 Homogeneous design experiments

Table 7 lists the experimental results of homogeneous design for surface roughness. Figure 8 is the scatter matrix plot of the surface roughness based on the experimental results of homogeneous design. The scatter plots show $R_{a,u}$ increases with cutting parameters increasing, and the value of $R_{a,u}$ is uniformly dispersed at different levels. It can be concluded that the interaction between cutting parameters has a significant influence on surface roughness ($R_{a,u}$). From the scatter plots of $R_{a,w,}$ it can be observed that $R_{a,w}$ is clearly divided into two parts. When the cutting parameters are all of high levels, such as v_c=502.72 m/min, f_z=0.07 mm/tooth, and a_p=2.0 mm, $R_{a,w}$ is larger. Therefore, the scatter plots of $R_{a,w}$ showed the same result as in Fig. 7, which was caused by the same reasons.

4 Surface roughness prediction model

Regression analysis method is used to establish the mathematical prediction model of surface roughness. In

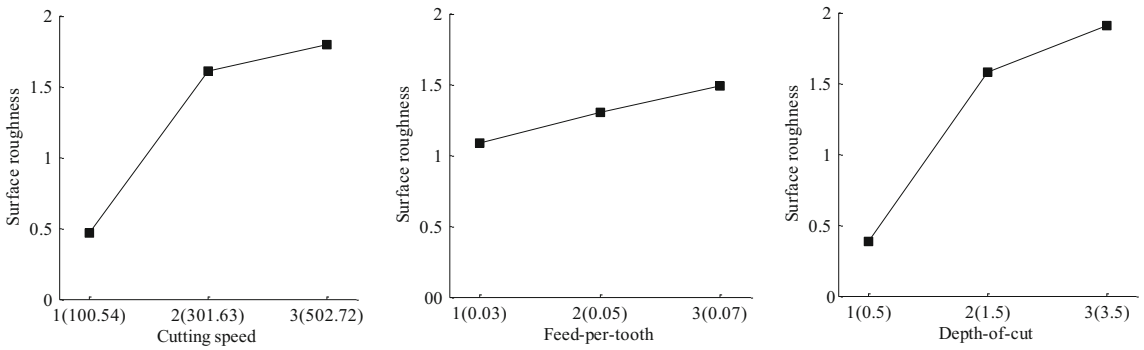

(a) Cuting speed **(b) Feed-per-tooth** **(c) Depth-of-cut**

Fig. 6 The main effects plots for $R_{a,w}$

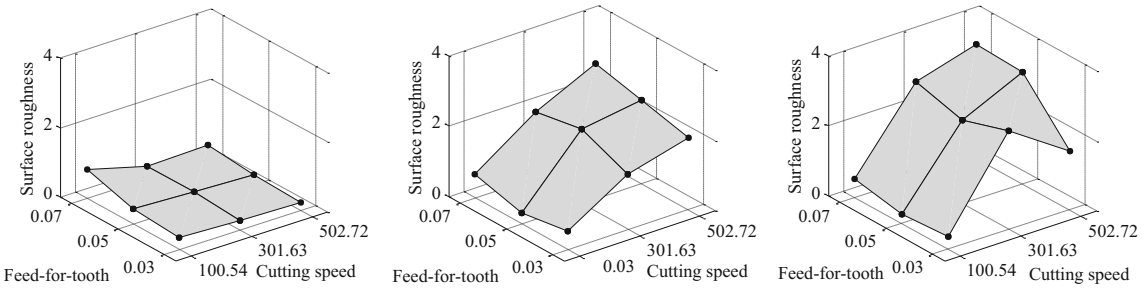

Fig. 7 Effect of spindle speed and feed per tooth on $R_{a,w}$ in different depth of cut

the presented investigation, a whole analysis was done using the experimental data in Tables 4 and 6. A non-linear polynomial model was performed to predict the surface roughness by the partial least square regression. The regression model can be expressed as

$$R_{a,j} = b_{0,j} + b_{1,j}v_c + b_{2,j}f_z + b_{3,j}a_p + b_{4,j}v_c f_z + b_{5,j}f_z a_p + b_{6,j}v_c a_p + b_{7,j}v_c^2 + b_{8,j}f_z^2 + b_{9,j}a_p^2 \quad (1)$$

where $R_{a,j}$ (j=u, w) is the surface roughness, $b_{i,j}$ (i=0, 1… 9) is the coefficient of the non-linear polynomial model, v_c is cutting speed (m/min), f_z is the feed per tooth (mm/tooth), and a_p is the depth of cut (mm). Let x_1=v_c, x_2=f_z, x_3=a_p, x_4=$v_c f_z$, x_5=$f_z a_p$, x_6=$v_c a_p$, x_7=v_c^2, x_8=f_z^2, and x_9=a_p^2, and then Eq. (1) can be written as follows:

$$R_{a,j} = b_{0,j} + b_{1,j}x_1 + b_{2,j}x_2 + b_{3,j}x_3 + b_{4,j}x_4 + b_{5,j}x_5 + b_{6,j}x_6 + b_{7,j}x_7 + b_{8,j}x_8 + b_{9,j}x_9 \quad (2)$$

Equation (2) is a multiple linear regression model. Table 8 lists the data for the prediction model of surface roughness.

The variable values of Table 8 are mean-centered and normalized before the regression calculation for Eq. (2). The mean-centered and normalized function is

$$x_{ij}^* = \left(x_{ij} - \overline{x_j}\right)/s_j = \left(x_{ij} - \overline{x_j}\right) \Big/ \sqrt{\frac{1}{n}\sum_{i=1}^{n}\left(x_{ij} - \overline{x_j}\right)^2} \quad (3)$$

where x_{ij} is the jth values of variable x_j, $\overline{x}_j$ is the mean of variable x_j, and s_j is the standard deviation.

Table 7 The experimental results of homogeneous design

No.	v_c [m/min]	f_z [mm/tooth]	a_p [mm]	$R_{a,u}$ [μm]	$R_{a,w}$ [μm]
1	100.54	0.03	1.0	0.212	0.342
2	201.09	0.04	2.5	0.367	0.374
3	402.18	0.05	0.5	0.229	0.383
4	502.72	0.07	2.0	0.693	3.572
5	100.54	0.04	1.5	0.337	0.319
6	301.63	0.05	2.0	0.450	2.288
7	301.63	0.06	1.5	0.447	0.434
8	502.72	0.07	0.5	0.397	0.414
9	201.09	0.03	0.5	0.248	0.318
10	201.09	0.03	2.5	0.447	0.312
11	402.18	0.06	1.0	0.331	2.720
12	402.18	0.06	2.0	0.664	2.833
13	301.63	0.05	1.0	0.291	0.265
14	502.72	0.07	2.5	0.625	3.245
15	100.54	0.03	2.0	0.279	0.341
16	201.09	0.04	0.5	0.186	0.327
17	402.18	0.05	2.5	0.599	2.891
18	502.72	0.07	1.0	0.418	0.618

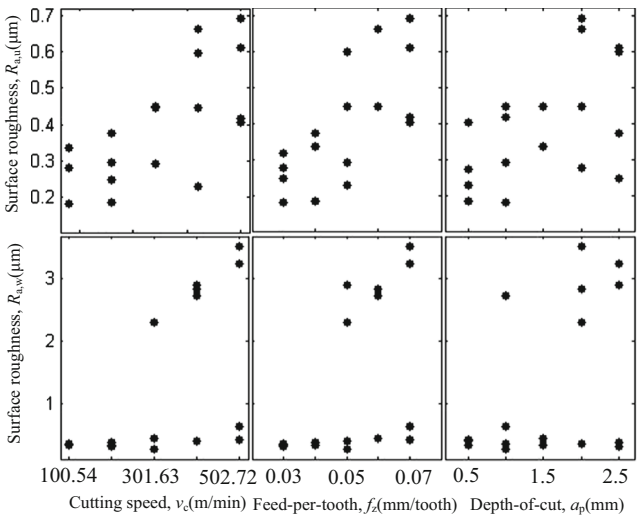

Fig. 8 The scatter matrix plot of surface roughness

Table 8 The data for prediction model

Experiment no.	x_1, (v_c)	x_2, (f_z)	x_3, (a_p)	x_4, ($v_c f_z$)	x_5, ($f_z a_p$)	x_6, ($v_c a_p$)	x_7, (v_c^2)	x_8, (f_z^2)	x_9, (a_p^2)	$R_{a,u}$	$R_{a,w}$
1	100.54	0.03	0.5	3.0162	0.015	50.27	10108.29	0.0009	0.25	0.260	0.326
2	301.63	0.03	0.5	9.0489	0.015	150.815	90980.66	0.0009	0.25	0.213	0.255
3	502.72	0.03	0.5	15.0816	0.015	251.36	252727.4	0.0009	0.25	0.181	0.237
–	–	–	–	–	–	–	–	–	–	–	–
44	402.18	0.05	2.5	20.109	0.125	1005.45	161748.8	0.0025	6.25	0.599	2.891
45	502.72	0.07	1.0	35.1904	0.07	502.72	252727.4	0.0049	1	0.418	0.618

The surface roughness regression equation can be calculated by the method of partial least square. Nine latent variables including in the surface roughness prediction model are selected based on the cross validation, and then the mean-centered and normalized regression model for surface roughness obtained as follows:

$$\begin{cases} R^*_{a,u} = 0.2010x^*_1 + 0.5301x^*_2 + 0.7582x^*_3 \\ \quad -0.0064x^*_4 + 0.1727x^*_5 + 0.2351x^*_6 \\ \quad -0.0663x^*_7 + 0.1566x^*_8 + 0.0274x^*_9 \\ R^*_{a,w} = 0.5668x^*_1 + 0.1020x^*_2 + 0.5879x^*_3 \\ \quad -0.0486x^*_4 + 0.0200x^*_5 + 0.4537x^*_6 \\ \quad -0.1414x^*_7 + 0.0138x^*_8 - 0.1516x^*_9 \end{cases} \tag{4}$$

where x_i^* is the mean-centered and normalized variable.

After original variables being mean-centered and normalized, the regression coefficients of Eq. (4) indicate the degree that the corresponding independent variables (cutting parameters) influence on the dependent variable ($R_{a,u}$ and $R_{a,w}$). The greater value of the regression coefficient indicates that the corresponding variable has greater significance for surface roughness ($R_{a,u}$, and $R_{a,w}$). The effect of variable coefficient meant positive effect, negative coefficient meant negative effects. Figure 9 shows the histogram of the coefficients of Eq. (4). From Fig. 9, the same results with the ANOVA for surface roughness ($R_{a,u}$ and $R_{a,w}$) can be concluded.

The mean-centered and normalized variables of Eq. (4) are converted into the original variables. Then the surface roughness prediction model is

$$\begin{cases} R_{a,u} = 0.4319 + 1.0144 \times 10^{-4} v_c - 11.209 f_z \\ \quad -0.0854 a_p - 4.2745 \times 10^{-4} v_c f_z + 3.2926 f_z a_p \\ \quad +3.2141 \times 10^{-4} v_c a_p - 5.9072 \times 10^{-7} v_c^2 \\ \quad +136.95 f_z^2 + 0.01 a_p^2, R^2 = 0.9313 \\ R_{a,w} = -0.7454 + 0.0038 v_c + 2.9394 f_z \\ \quad +0.5999 a_p - 0.0219 v_c f_z + 1.8352 f_z a_p \\ \quad +4.2876 \times 10^{-3} v_c a_p - 8.6547 \times 10^{-6} v_c^2 \\ \quad +82.039 f_z^2 - 0.3745 a_p^2, R^2 = 0.9257 \end{cases} \tag{5}$$

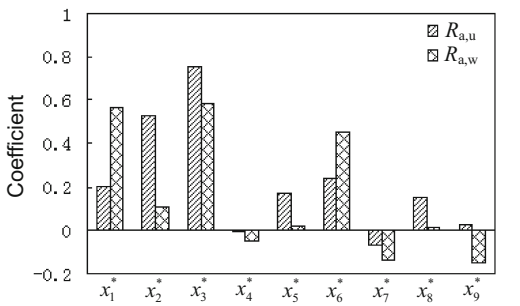

Fig. 9 Coefficients of the mean-centered and normalized regression model

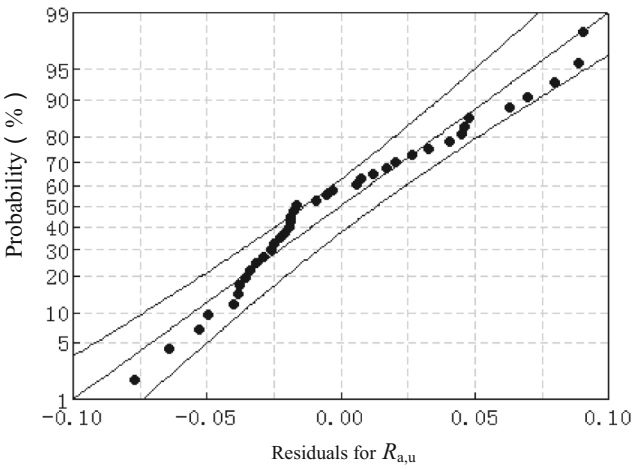

(a) Residuals for $R_{a,u}$

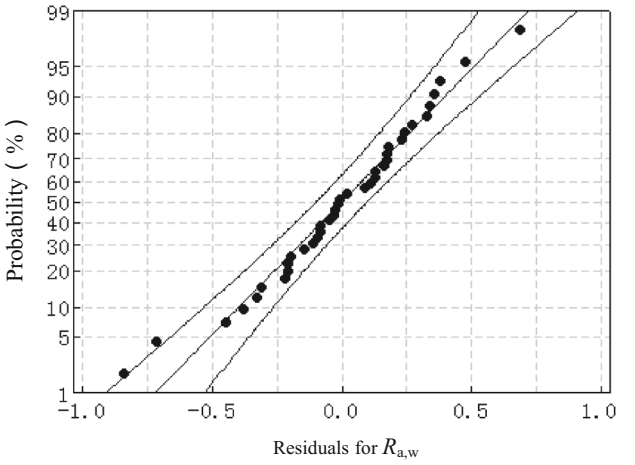

(b) Residuals for $R_{a,w}$

Fig. 10 Normal probability plot of residuals (5 % confidence interval)

Table 9 The results of confirmation experiments

No.	v_c [m/min]	f_z [mm/tooth]	a_p [mm]	$R_{a,u}$ [μm]			$R_{a,w}$ [μm]		
				Experimental	Predicted	Error (%)	Experimental	Predicted	Error (%)
1	100.53	0.03	1.2	0.265	0.291	9.81	0.382	0.409	7.07
2	201.06	0.07	1.5	0.595	0.646	8.57	1.318	1.511	14.64
3	301.59	0.04	0.8	0.312	0.295	5.45	0.835	0.932	11.62
4	387.46	0.05	0.7	0.328	0.304	7.32	0.726	0.819	12.81
5	502.65	0.06	1	0.407	0.425	4.23	1.175	1.279	8.85

Error=|(experimental predicted)/experimental|×100 %

where R^2 is the coefficient of multiple determination. This value indicates that the presented model fits the data very well. Figure 10 shows the normal probability plot of residuals for the regression model. It can be easily observed that the residuals do not appear abnormally and the plot appears linear. In order to verify the accuracy of the proposed surface roughness prediction model, five experiments were performed at the same experimental condition as designed previously. The predicted value and the associated experimental value were compared and the percentage error was calculated. Table 9 shows the results of experiments. It can be concluded that the error percentage is within the permissible limits. The biggest error are 9.81 % for $R_{a,u}$ and 14.64 % for $R_{a,w}$. So, the prediction model of surface roughness is accurate and credible, and it can be used to predict the surface roughness values at any cutting speed, feed per tooth, and depth of cut within the range of the experimentation conducted.

5 Conclusion

The following conclusions can be concluded based on the experimental results in the high-speed peripheral milling of ALMn1Cu:

(1) The range analysis of factorial experiment indicates that the minimum $R_{a,u}$ and $R_{a,w}$ are all achieved at v_c=502.72 *m*/min, f_z=0.03 mm/tooth, and a_p=0.5 mm. In this experimental condition, the same cutting experiments were carried out four times, the $R_{a,u}$ is within 0.145~0.187 μm and the $R_{a,w}$ is within 0.210~0.245 μm.

(2) The significant factors affecting $R_{a,u}$ are the depth of cut, feed per tooth, cutting speed, and interaction between cutting speed and depth of cut. The most statistically significant factor influencing on $R_{a,u}$ is the depth of cut, which explains 52.53 % of the total variances. The second largest contribution comes from the feed per tooth with 11.403 %.

(3) The significant factors affecting $R_{a,w}$ are the depth of cut, cutting speed, and interaction between cutting speed and depth of cut. The depth of cut is the most statistically significant factor which explains 38.08 % of the total variances. The second largest contribution comes from the cutting speed with 30.71 %, and the feed per tooth does not have statistical significance on $R_{a,w}$. The conditions to obtain the smaller values of $R_{a,w}$ are high cutting speed, small feed per tooth, and small depth of cut.

(4) The non-linear polynomial model of surface roughness based on the cutting parameters was built by the method of partial least square, and the R^2 values for the mathematical prediction model of surface roughness is enough to obtain reliable estimates. The further validation experiments show that the experimental values of surface roughness well correspond to the prediction. So, the proposed mathematical prediction model of surface roughness can be used to estimate the expected performance for any factor levels.

Acknowledgments The project is supported by the National Natural Science Foundation of China (51105207).

References

1. Benardos PG, Vosniakos G-C (2003) Prediction surface roughness in machining: a review. Int J Mach Tool Manuf 43:833–844
2. Geoffrey B, Winston AK (1989) Fundamentals of machining and machine tools. Marcel dekker, INC, New York, US
3. Fang XD, Sfai-Jahanshaki H (1997) A new algorithm for developing a reference model for prediction surface roughness in finish machining of steels. Int J Prod Res 35:179–197
4. Hasan Ö, Tuncay E, Mustafa Ç (2006) A study of the Taguchi optimization method for surface roughness in finish milling of mold surfaces. Int J Adv Manuf Technol 28:694–700
5. Chen JC, Lee SS (2003) An on-line surface roughness recognition system using an accelerometer in turning operations. J Eng Technol 20:12–18
6. El-Axir MH, Othman OM, Abodiena AM (2008) Study on the inner surface finishing of aluminum alloy 2014 by ball burnishing process. J Mater Process Technol 202:435–442
7. Erol K, Mesut H, Ahmet Y (2011) Prediction and analysis of surface roughness characteristics of a non-ferrous material using ANN in CNC turning. Int J Adv Manuf Technol 52:79–88

8. Wang SJ, To S, Cheung CF (2013) An investigation into material-induced surface roughness in ultra-precision milling. Int J Adv Manuf Technol 68:607–616
9. Cakir CM, Ensrioglu C, Demirayak I (2009) Mathematical modeling of surface roughness for evaluating the effects of cutting parameters and coating material. J Mater Process Technol 209:102–109
10. Chinnasamy NS, Muthu PK (2011) Optimization of drilling parameters on surface roughness in drilling of AISI 1045 using response surface methodology and genetic algorithm. Int J Adv Manuf Technol 57:1043–1051
11. Karayel D (2009) Prediction and control of surface roughness in CNC lathe using artificial neural network. J Mater Process Technol 209:3125–3137
12. Huang BP, Chen JC, Li Y (2008) Artificial-neural-networks-based surface roughness Pokayoke system for end-milling operations. Neurocomputing 71:544–549
13. Öktem H (2009) An integrated study of surface roughness for modelling and optimization of cutting parameters during end milling operation. Int J Adv Manuf Technol 43:852–861
14. Lee BY, Liu HS, Tarng YS (1998) Modeling and optimization of drilling process. J Mater Process Technol 74:149–157
15. Çolak O, Kurbanoglu C, Kayacan MC (2007) Milling surface roughness prediction using evolutionary programming methods. Mater Des 28:657–666
16. Ding TC, Zhang S, Wang YW, Zhu XL (2010) Empirical models and optimal cutting parameters for cutting forces and surface roughness in hard milling of AISI H13 steel. Int J Adv Manuf Technol 51:45–55
17. Basak H, Goktas Haldun H (2009) Burnishing process on Al-alloy and optimization of surface roughness and surface hardness by fuzzy logic. Mater Des 30:1275–1281
18. Oktem H, Erzurumlu T, Erzincanli F (2006) Prediction of minimum surface roughness in end milling mold parts using neural network and genetic algorithm. Mater Des 27:735–744
19. Bozdemir M, Aykut Ş (2012) Optimization of surface roughness in end milling Castamide. Int J Adv Manuf Technol 62:495–503
20. Palani S, Natarajan U (2011) Prediction of surface roughness in CNC end milling by machine vision system using artificial neural network based on 2D Fourier transform. Int J Adv Manuf Technol 54:1033–1042
21. Dhokia VG, Kumar S, Vichare P, Newman ST (2008) An intelligent approach for the prediction of surface roughness in ball-end machining of polypropylene. Robotics Comput-Integ Manuf 24:835–842
22. Lu C (2008) Study on prediction of surface quality in machining process. J Mater Process Technol 205:439–450
23. Benardos PG, Vosniakos GC (2002) Prediction of surface roughness in CNC face milling using neural networks and Taguchi's design of experiments. Robot Comput Integ Manuf 18:343–354
24. Çaydaş U, Hasçalik A (2008) A study on surface roughness in abrasive waterjet machining process using artificial neural networks and regression analysis method. J Mater Process Technol 202:574–582
25. EI-Sonbaty IA, Khashaba UA, Selmy AI, Ali AI (2008) Prediction of surface roughness profiles for milled surface using an artificial neural network and fractal geometry approach. J Mater Process Technol 200:271–278